Vol. 38 No. 3 Journal of the Communications Research Laboratory November 1991
Printed in Tokyo, Japan pp. 543 – 551

IV. EXPERIMENTAL RESULTS

IV 4. GEODETIC RESULTS FROM DOMESTIC VLBI EXPERIMENTS (2) MINAMI-TORISHIMA (MARCUS) EXPERIMENTS

By
Yasuhiro KOYAMA

(Received on March 18, 1991)

ABSTRACT

Minami-Torishima (Marcus Reef) VLBI station has been in operation since 1989, being used for geodetic VLBI experiments in both 1989 and 1990. This paper describes the format and results of the two recent experiments held in 1990.

By analyzing both the X-band and S-band time delay data from each experiment, the position of the VLBI reference point of Minami-Torishima station has been determined precisely with an inherent uncertainty of about 3 cm in a geocentric Cartesian coordinate system. These results provide the first geodetic position for the Minami-Torishima VLBI station, in the sense that ionospheric delay corrections were successfully applied to the obtained data. A new method of rejecting bad data from a set of observation data was employed by calculating "closure delay" from three time-delay values of three baselines making up a triangle. This method was used in place of the conventional one based on "quality code", since the crystal-cesium system used as a frequency standard at the Minami-Torishima station is inferior in stability to the hydrogen maser system used at the other stations. Although the differences between the VLBI station's three dimensional components from two experiments are around 10 cm, estimated lengths for baselines showed good agreement within the 2 cm uncertainty for each experiment.

1. Introduction

A Western Pacific VLBI Network (WPVN) was proposed by the Communications Research Laboratory (CRL) to study relative plate motions between four tectonic plates around the Japanese Archipelago. These motions are to be examined by performing a series of precise measurements using a Geodetic VLBI technique[1]. The WPVN project actually began in 1988 and the Minami-Torishima VLBI station has been operating as a WPVN observation station since 1989. Figure 1 shows the location of four VLBI stations in WPVN and boundaries between the four tectonic plates with which the project is concerned. Each plate is moving independently and producing complicated interactions with other plates at these boundaries. It is well known that the distribution of seismic centers is quite dense at such plate boundaries, which strongly suggests relations between the mechanisms of earthquakes and the dynamics of tectonic plate motions. It can be considered that most earthquakes occurring in the region around the

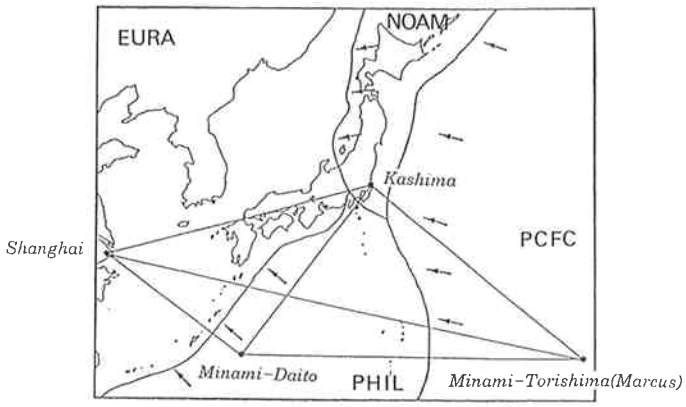

Fig. 1 Western Pacific VLBI Network. The four VLBI stations are indicated by dots along with their station names. Note that each of these four stations are located on a different plate, the four plates being NOAM (North American Plate), PCFC (Pacific Plate), EURA (Eurasian Plate) and PHIL (Philippine Plate). Plate motion directions relative to the Eurasian Plate expected from a plate motion model are also indicated by arrows.

Japanese Archipelago are triggered by the complicated interactions between the surrounding four plates, and it is the goal of WPVN to provide useful information for the study of seismic mechanisms and earthquake prediction. As shown in Fig. 1, each VLBI station in WPVN is located on one of the four tectonic plates, no two stations on the same plate. This network configuration is effective since the relative movements between these plates can be investigated by monitoring the length of baselines between VLBI stations, which are direct outputs of a geodetic VLBI experiment.

Ground facilities for the Minami-Torishima VLBI station including a 10m-diameter antenna were constructed in 1989 in the north-east part of the island. Facilities of the Japanese Maritime Self-Defense Force and Japanese Meteorological Agency are also located here [2]. At the same time, a multifrequency 34m-diameter antenna was also constructed at Kashima Space Research Center (KSRC) of CRL. At KSRC, CRL has another VLBI station with a 26-meter antenna used for geodetic VLBI experiments since 1983. KSRC thus has two VLBI stations available for use. Shanghai Observatory of the Chinese Academy of Sciences joins the WPVN project with a 25-meter antenna constructed in 1985 at Seshan station located on the Eurasian Plate. In the experiments discussed in this paper, these four antennas were involved.

The first VLBI experiment utilizing WPVN was conducted in 1989 using only three stations: Minami-Torishima, Kashima (26-meter antenna) and Shanghai stations. However, at that time, the quality of S-Band data obtained from baselines including Minami-Torishima station were poor. This was because phase calibration signals in S-band frequency channels were affected by radio frequency interference seemingly generated from a phase-locked oscillator for the X-band receiver of the antenna[3]. Since S-band data in VLBI experiments are important for ionospheric delay corrections to X-band data, results from the first experiment were not good enough to precisely determine the position of Minami-Torishima station. Therefore, for the experiments held in 1990, the observation channel frequencies were chosen carefully so that the phase calibration signal was not contaminated by spurious signals. By analyzing the data obtained from these 1990 experiments, the position of the Minami-Torishima station was determined precisely for the first time. Details and results of the analysis applied to the two experiments in 1990 are

presented and discussed in this paper.

2. Experiments

2.1 Overview of Experiments

There were two experiments held in 1990 with the Minami-Torishima station as listed in Table 1. Each experiment was performed with a set of observations spanning roughly 24 hours. Four VLBI stations: the 26-meter antenna at Kashima (KA26), the 34-meter antenna at Kashima (KA34), the 10-meter antenna at Minami-Torishima (MRCS) and the 25-meter antenna at Seshan (SESH), participated in both of these experiments. In addition to the four stations, the 26-meter antenna station at Fairbanks, Alaska (FBNK) joined the first experiment coded as MRCS-3 in the table. Every station except for the Minami-Torishima station was equipped with a hydrogen-maser clock as a frequency standard. For the Minami-Torishima station, a combined system consisting of a highly stable crystal oscillator and a Cesium-beam clock[4] was transported temporarily to the site for the frequency standard system. The Cesium-beam clock was kept operating during transportation from CRL to the remote observation site. A Mark-III VLBI data acquisition terminal was employed as a back-end system at the Seshan station with a wide-track normal-density data recorder and also at the Fairbanks station with a narrow-track high-density data recorder. K-4 VLBI data acquisition terminals developed by CRL were employed at the Kashima 26-meter antenna station and at the Minami-Torishima station [5],[6]. At the Kashima 34-meter antenna station, a K-3 VLBI data acquisition terminal was used as a back-end system for both experiments, although the data recorder was different for each experiment. A K-3 type, narrow-track high-density data recorder was used for experiment MRCS-3, while a K-4 data recorder was used for the second experiment, MRCS-4.

Table 1 Minami-Torishima VLBI experiments in 1990

CODE	Start Time (UT)–End Time (UT)	Participated Stations
MRCS-3	June 25, 16:00–June 26, 16:02	KA34, KA26, MRCS, SESH, FBNK
MRCS-4	June 30, 00:21–June 30, 23:54	KA34, KA26, MRCS, SESH

2.2 Observations

As in usual geodetic VLBI experiments, each experiment consisted of individual observations towards common radio sources among the participating VLBI stations. In each of the two experiments, 18 sources were observed repeatedly for 24 hours. Since the cesium-crystal frequency standard system was employed at the Minami-Torishima station, integration time for cross correlation of each observation was restricted to obtain an optimum signal-to-noise ratio. From the study of coherence loss due to instability of the frequency standard system[4], 120 seconds of integration is considered to be favorable. By taking account of the time necessary for tape synchronization at correlation processing, one fourth of the recording time (196 seconds) of Mark-III tapes was chosen as the actual observation time. Since the

Table 2 List of Sources

Source Name	Right Ascension (J2000.0)	Declination (J2000.0)
0212 + 735	$02^h17^m30.81378^s$	+73°49'32.62119"
0234 + 285	02 37 52.40574	+28 48 08.98930
0420 – 014	04 23 15.80069	–01 20 33.06586
0528 + 134	05 30 56.41676	+13 31 55.14816
0552 + 398	05 55 30.80563	+39 48 49.16316
0727 – 115	07 30 19.11242	–11 41 12.60165
0472 + 103	07 45 33.05938	+10 11 12.69019
OJ287	08 54 48.87488	+20 06 30.63929
4C39.25	09 27 03.01380	+39 02 20.85046
3C273B	12 29 06.69970	+02 03 08.59916
*1334 – 127	13 37 39.78278	–12 57 24.70040
OQ208	14 07 00.39432	+28 27 14.69060
*1611 + 343	16 13 41.06416	+34 12 47.90930
NRAO530	17 33 02.70578	–13 04 49.54477
1803 + 784	18 00 45.68370	+78 28 04.02047
1921 – 293	19 24 51.05590	–29 14 30.11664
2121 + 053	21 23 44.51740	+05 35 22.09582
2234 + 282	22 36 22.47092	+28 28 57.41496

* These sources are not included in GLB401 Solution.

integration time for each observation was limited and the correlated amplitude was also expected to be degraded by a loss of coherence due to instability of the frequency standard system, it was necessary to choose strong sources as objects of observations. The radio sources observed during the experiments are listed in Table 2. Except for 1334 – 127 and 1611 + 343, all other sources had been repeatedly observed in VLBI experiments under the Crustal Dynamics Project (CDP) and the coordinates of each sources were obtained from a report on these experiments[7]. The coordinates of sources used in the analysis are also listed in the table.

2.3 Observing Frequency Sequences

Channel assignment for the observing frequencies in the experiments was basically the same as that of two WPVN experiments performed in 1989 or that of other usual CDP experiments. For X-band, eight channels of observing frequencies were assigned and the remaining six channels were assigned to S-band. Bandwidth of each channel was also the same (2 MHz). However, local frequency for each channel was set differently from the two experiments in 1989 but the same as in CDP experiments. For the experiments in 1989, the frequency sequence was restricted due to the type of K-4 video converter component in use at the Minami-Torishima at that time. Each local frequency had to be chosen as $N \times 10 + 9.99$ MHz, where N is an integer. Moreover, because of this frequency sequence, every phase calibration signal in S-band observing channels experienced strong interference which seemed to radiated from the phase-locked oscillator of the X-band receiver. Therefore, S-band data, which are important for corrections in ionospheric propagation delay, were not available for the baselines including Minami-Torishima station. By enabling the K-4 type video converter set to set local frequencies with 1 MHz steps as $N + 0.99$ MHz, it became possible to use the frequency sequences shown in Table 3.

Table 3 List of observation frequencies

Channel #	Local Frequency (MHz)
1	8210.99
2	8220.99
3	8250.99
4	8310.99
5	8420.99
6	8500.99
7	8550.99
8	8570.99
9	2217.99
10	2222.99
11	2237.99
12	2267.99
13	2292.99
14	2302.99

2.4 Correlation Processing

Because the CRL correlation system available at KSRC at present does not accept high density tapes from K-3 or Mark-III high-density recorders, observation tapes recorded at the KA34 and FBNK VLBI stations in experiment MRCS-3 were not processed at KSRC. These tapes were sent to the Washington Correlation Center of United States Naval Observatory for correlation processing. In this paper, correlated data processed only at KSRC were used for analysis and discussion, and hence there are three sets of baseline data for MRCS-3 and six sets for MRCS-4.

3. Analysis of Data and Geodetic Results

After a geodetic VLBI experiment, recorded signal data received at different antennas are processed by a correlator to obtain time delays and their time derivatives, i.e., delay rates. The time delay is defined by the interval between the time when one antenna receives a signal from a radio source and the time when another antenna receives the same signal from the same radio source. If instability of a frequency standard system is not considered, estimated uncertainties for time delay ($\sigma(\tau)$) and delay rate ($\sigma(\dot{\tau})$) can be expressed as[8],

$$\sigma(\tau) = \frac{1}{2\pi B_e \cdot \mathrm{SNR}} \qquad \cdots\cdots (1)$$

$$\sigma(\dot{\tau}) = \frac{\sqrt{12}}{2\pi f T \cdot \mathrm{SNR}} \qquad \cdots\cdots (2)$$

where T is the integration time and B_e is the effective bandwidth. The effective bandwidth is determined as the square root of frequencies assigned to each observation channel. In the frequency sequence of Table 3, B_e is 140.2 MHz and 33.1 MHz for X-band and S-band, respectively. SNR is the signal-to-noise ratio

which varies with each observation according to the strength of the observed source and also to integration time. As can be seen from the equations, delay rate uncertainty is inversely proportional to integration time T, whereas time delay uncertainty is only an indirect function of T through SNR. If the integration time is limited as in the case of MRCS-3 and MRCS-4, delay rate uncertainty become large.

In addition to the uncertainties expressed by Eqs. (1) and (2), instability of the cesium-crystal system should be taken into account as another source of error, especially for delay rate. According to a measurement[(4)], the Allan variance of the cesium-crystal system for 120 sec is approximately 3×10^{-13}, which is larger than 5.5×10^{-14} (sec/sec), the uncertainty in delay rate calculated from Eq. (2) for X-band using 120 seconds for T and 10 for SNR. Although the value of SNR varies according to the strength of the source, SNR = 10 was a typical case for the KA26-MRCS baseline. On the other hand, the error in time delay ε_τ due to the instability of the frequency standard system can be evaluated as the product of the Allan variance σ_y and the integration time T:

$$\varepsilon_\tau = \sigma_y \times T \qquad (3)$$

This equation gives an ε_τ of 3.6×10^{-11} (sec) for an integration time of 120 seconds. This error is smaller than the uncertainty in time delay calculated from Eq. (1), which is 1.1×10^{-10} (sec) for X-band with SNR = 10. Therefore, the effects of instability in the frequency standard system is much greater for delay rate than for time delay. Consequently, only the data set for time delay was used for the analysis treated in this paper.

Once a set of time delay data is obtained after correlation processing, the validity of each value must be judged before baseline analysis. A wrong peak in the cross-correlation function is sometimes detected and such data should be rejected from the data set. In most VLBI experiments, a measure called "quality code" is used to perform data validation. Quality code is calculated for each result of a correlation, based on a fluctuation in correlated amplitude. If the correlation amplitude fluctuates during the integration time, the quality code is set to a lower number. Although, this measure is useful to observe the quality of data in an easy fashion, it does not reflect the true quality of data when a frequency standard system is not sufficiently stable. When a standard frequency signal at one station changes its frequency, correlated amplitude fluctuates and hence the quality code will be inadequately set. Since the experiments treated here employed the Cesium-Crystal system at the Minami-Torishima station, a measure of "closure delay" was calculated and employed to evaluate data quality. The closure delay (τ_Δ) is defined by Eq. (4):

$$\tau_\Delta = \tau_{12} - \tau_{13} + \tau_{23} + \tau_{12} \times \dot{\tau}_{23} \qquad (4)$$

where τ_{ij} is time delay between the i'th station and j'th station and $\dot{\tau}_{ij}$ is delay rate. The closure delay can be calculated from any set of three baselines composed from three stations. If time delay of one baseline is not a good datum, then closure delay including the baseline will have a large absolute value. If closure delay is close to zero, it is highly probable that all three baseline data can be used for the analysis. Figure 2 shows a histogram of closure delay calculated from MRCS-3 and MRCS-4 with three station (1:KA26, 2:MRCS, and 3:SESH). It can be seen from the figure that closure delay is normally distributed around zero, while its absolute value sometimes exceeds 0.1 nanosecond, which is outside the normal distribution. In the analysis, only time delay data with small absolute values of closure delay, i.e. less than 0.1 nanosecond, were used.

Table 4 summarizes the results from the analysis. In this analysis, ionospheric delay corrections were applied from the differences in time delay between X-band and S-band. To correct tropospheric

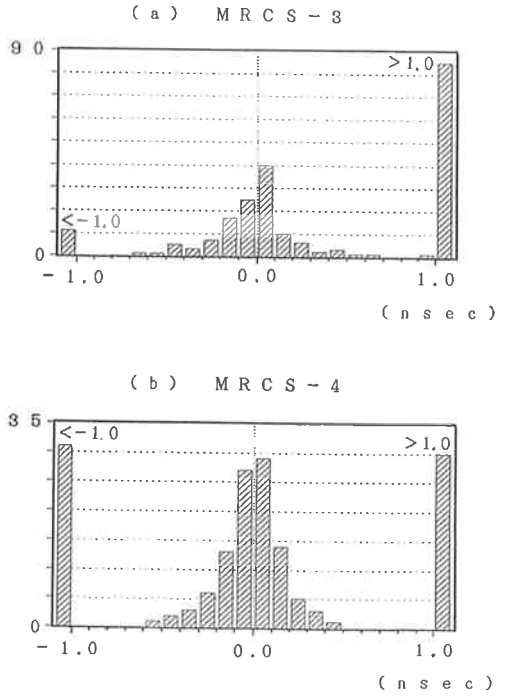

Fig. 2 Histogram of closure delay calculated for KA26-MRCS-SESH for (a) experiment MRCS-3 and (b) experiment MRCS-4.

Table 4(a) Estimated positions

Station		MRCS-3	MRCS-4	Difference
KA26	X	–3997890.335m	–3997890.335m	
	Y	3276580.525m	3276580.525m	
	Z	3724118.788m	324118.788m	
KA34	X		–3997647.330m	
	Y		3276690.014m	
	Z		3724279.387m	
MRCS	X	–5227444.865 ± 0.044m	–5227444.950 ± 0.033m	8.5cm
	Y	2551378.606 ± 0.030m	2551378.730 ± 0.022m	12.4cm
	Z	2607605.338 ± 0.037m	2607605.398 ± 0.027m	6.0cm
SESH	X	–2831684.776 ± 0.034m	–2831684.693 ± 0.022m	8.3cm
	Y	4675732.961 ± 0.028m	4675732.888 ± 0.020m	7.3cm
	Z	3275328.213 ± 0.033m	3275328.257 ± 0.022m	4.4cm

Table 4(b) Estimated baselines

Baseline	MRCS-3	MRCS-4	Difference
KA34-MRCS		1812578.120 ± 0.013m	
KA34-SESH		1875725.713 ± 0.008m	
KA26-MRCS	1812270.509 ± 0.015m	1812270.480 ± 0.013m	2.9cm
KA26-SESH	1875920.034 ± 0.014m	1875920.020 ± 0.008m	1.4cm
MRCS-SESH	3270841.125 ± 0.018m	3270841.117 ± 0.014m	0.8cm

propagation delay, the dry troposphere component was calculated from the CFA2.2 model[9] using ground weather data. Both the wet tropospheric components and clock difference were estimated with a continuously changing model using a linear term, and a constraint of 50 psec/sec was applied for the change in wet tropospheric delay[10]. Since the position of the 26-meter antenna at Kashima has been frequently measured by VLBI experiments, it was not estimated but fixed throughout the analysis. The position of the 34-meter antenna at Kashima was also fixed by calculating it from vector components of the 26 m–34 m baseline which had been independently obtained by VLBI experiments[11].

4. Future Analyses and Experiments

As described in section 2, data from the Kashima 34 m antenna station and Fairbanks station were not included in the MRCS-3 analysis. By adding these data, additional baseline delay data can be used for closure delay calculation to identify bad observations. After all data becomes available, a total set of delay data will be combined and analyzed to provide one unified data base from the two VLBI experiments.

To determine the direction and velocity of the Minami-Torishima VLBI station precisely, more VLBI experiments must be performed after an adequate interval, for example, one year. For this purpose, Geodetic VLBI experiments including the Minami-Torishima station are now considered to be scheduled at least once a year until 1993. In addition to our baseline research, continuous 168 hour (7 days) VLBI experiments for tropospheric and ionospheric modeling studies are now under consideration.

Acknowledgements

The author would like to thank all the members at Kashima Space Research Center, Shanghai Observatory and Fairbanks Observatory for the observations they performed and for their helpful suggestions and comments. The observations at Minami-Torishima station were largely supported by the Japanese Maritime Self-Defense Force and Japanese Meteorological Association.

References

(1) M. Imae, "Domestic VLBI Experiments at the Communications Research Laboratory", J. Commun. Res. Lab., (II.2 of this issue).

(2) S. Hama and J. Amagai, "10 m antenna for Minami-Torishima (MARCUS) Isl." (in Japanese), Rev. Commun. Res. Lab., vol. 36 Special Issue No. 8, p. 61, 1990.

(3) Y. Takahashi, J. Amagai, and S. Hama, "The First VLBI Experiment of Western Pacific VLBI

Network" (in Japanese), Rev. Commun. Res. Lab., vol. 36, Special Issue No. 8 p. 141, 1990.

(4) H. Kiuchi, J. Amagai, N. Kawaguchi, "A Highly Stable Crystal Oscillator Applied to Geodetic VLBI", J. Commun. Res. Lab., vol. 36, p. 107, 1989.

(5) H. Kiuchi, J. Amagai, and Y. Abe, "A New VLBI Data Acquisition System, K-4" (in Japanese), Rev. Commun. Res. Lab., vol. 36, Special Issue No. 8 p. 79, 1990.

(6) S. Hama, H. Kiuchi, and J. Amagai, "The K-4 High Density Data Recorder" (in Japanese), Rev. Commun. Res. Lab., vol. 36, Special Issue No. 8, p. 91, 1990.

(7) C. Ma, J. W. Ryan, and D. Caprette, "Crustal Dynamics Project Data Analysis–1988", NASA Technical Memorandum 100723, 1989.

(8) N. Kawagushi, "Coherence Loss and Delay Observation Error in Very Long Baseline Interferometry", J. Radio Res. Lab., vol. 30, No. 129, p. 59, 1983.

(9) J. L. Davis, T. A. Herring, I. I. Shapiro, A. E. E. Rogers, and G. Elgered, "Geodesy by Radio Interferometry: Effects of Atmospheric Modelling Errors on Estimates of Baseline Length", Radio Science, vol. 20, p. 1593, 1985.

(10) K. Heki, "Three Approaches Toward the Better Estimation of Vertical VLBI Station Positions", Proc. Japanese Symposium on Earth Rotation, Astronomy, and Geodesy (1989), p. 161, 1990.

(11) Y. Koyama, J. Amagai, and H. Kiuchi, "Precise Position Determination of New VLBI Station at Kashima", J. Commun. Res. Lab., (in press)